TiS Trends in Sciences
TRENDS IN SCIENCES 2027; 24(1): 14070
SPRINT Scholarly Publishing and Repository Integration Center
https://doi.org/10.48048/tis.2027.14070
RESEARCH ARTICLE

Optimizing Transfection Conditions to Enhance BMP-2 Expression in Umbilical Cord–Derived Mesenchymal Stem Cells

Nuzli Fahdia Mazfufah[1,2], Retno Wahyu Nurhayati[2,3,*], Maulana Dias Pratama[2], Ismail Hadisoebroto Dilogo[2,4,5] and Delvac Oceandy[6]

[1]Doctoral Program in Biomedical Sciences, Faculty of Medicine, Universitas Indonesia, Jakarta 10430, Indonesia
[2]Stem Cell and Tissue Engineering Research Center, Indonesia Medical Education and Research Institute, Faculty of medicine, Universitas Indonesia, Jakarta 10430, Indonesia
[3]Department of Chemical Engineering, Faculty of Engineering, Universitas Indonesia, West Java 16424, Indonesia
[4]Department of Orthopedic and Traumatology, Faculty of Medicine, Universitas Indonesia, Dr. Cipto Mangunkusumo National General Hospital, Jakarta 10430, Indonesia
[5]Stem Cell Medical Technology Integrated Service Unit, Dr. Cipto Mangunkusumo National General Hospital, Jakarta 10430, Indonesia
[6]Division of Cardiovascular Science, Manchester Academic Health Science Center, The University of Manchester, Manchester M139PL, United Kingdom

([*]Corresponding author's e-mail: retno.wahyu01@ui.ac.id)

Received: 13 April 2026, Revised: 18 May 2026, Accepted: 28 May 2026, Published: 30 July 2026

Abstract

Bone defects remain a major challenge in regenerative medicine due to their limited capacity for spontaneous healing. UC-MSCs represent a promising cell source for bone regeneration; however, their therapeutic potential can be further enhanced through gene delivery strategies that promote osteogenic factor expression, such as BMP-2. Nevertheless, efficient gene delivery into MSCs remains challenging due to low transfection efficiency and potential cytotoxicity. This study aimed to systematically optimize transfection conditions in UC-MSCs to enhance BMP-2 expression including transfection reagents, DNA-to-reagent ratios, and cell passage numbers while maintaining cell viability and phenotypic stability. Transfection efficiency was evaluated using GFP reporter expression through fluorescence microscopy and flow cytometry, while BMP-2 mRNA expression was assessed by qRT-PCR at mRNA level and ELISA at protein level. Cell viability was determined using the Trypan Blue exclusion assay. Among the tested reagents, Lipofectamine™ 3000 demonstrated the highest transfection efficiency (~9% - 10%) with acceptable cytotoxicity (~86%). Further optimization identified a ratio of 4.5 µL Lipofectamine™ 3000 to 2.5 µg plasmid DNA as the most effective condition, producing the highest BMP-2 mRNA expression (~2.7-fold increase) and protein secretion (~245 pg/mL). Additionally, lower passage cells (passage 2) exhibited significantly higher transfection efficiency and BMP-2 expression compared to higher passages. Importantly, UC-MSCs maintained their characteristic MSC surface markers (CD73, CD90, CD105) following transfection. In conclusion, optimized transfection conditions significantly improve BMP-2 expression in UC-MSCs while preserving cell viability and phenotype. These findings provide a reproducible strategy to enhance MSC-based gene delivery systems and support their potential application in bone regeneration and regenerative medicine.

Keywords: Mesenchymal Stem Cells (MSCs), Umbilical cord–derived MSCs (UC-MSCs), Bone morphogenetic protein-2 (BMP-2), Gene delivery, Transfection optimization, Osteogenic differentiation, Regenerative medicine

Introduction

Bone defects caused by trauma, tumor resection, congenital abnormalities, or degenerative diseases remain a major challenge in orthopedic and reconstructive medicine due to the limited regenerative

capacity of large or critical-sized bone defects [1-3]. Gold standard conventional treatments, including autografts and allografts, present several limitations such as donor site morbidity, restricted tissue availability, risk of immune rejection, and potential disease transmission [4,5]. Consequently, regenerative strategies based on mesenchymal stem cells (MSCs) have attracted increasing attention because of their self-renewal capacity, multilineage differentiation potential, and immunomodulatory properties [6,7]. Among various MSC sources, umbilical cord–derived MSCs (UC-MSCs) represent a particularly promising candidate due to their non-invasive collection procedure, high proliferative capacity, low immunogenicity, and ability to secrete bioactive factors involved in tissue repair [8,9].

Recent advances in regenerative medicine have shifted the therapeutic focus from direct cell transplantation toward cell-free approaches utilizing MSC-derived secretomes and exosomes [10-12]. Compared to cell-based therapies, these acellular derivatives offer practical advantages in terms of safety, stability, and ease of storage, while retaining therapeutic efficacy through their bioactive components, including cytokines, chemokines, and growth factors [13-15]. However, the intrinsic osteogenic potential of MSC-derived secretome remains relatively limited because MSCs naturally produce only low levels of osteoinductive factors, particularly bone morphogenetic protein-2 (BMP-2) [16]. BMP-2 plays a central role in osteogenic differentiation and bone regeneration [17,18], yet the clinical application of recombinant BMP-2 is restricted by its short biological half-life, high production cost, and risk of adverse effects when administered at high doses [19,20]. Therefore, enhancing endogenous BMP-2 production in UC-MSCs secretome through genetic engineering may represent a more effective, sustained, and clinically safer strategy to improve osteogenic capacity of MSCs [21-23].

The clinical and translational potential of genetically modified MSCs remains limited by inefficient and inconsistent gene delivery. Like other primary cells, MSCs exhibit intrinsic resistance to transfection, resulting in low transfection efficiency and heterogeneous gene expression profiles [24,25]. Successful nuclear delivery and transcription of plasmid DNA (pDNA) in MSCs depend on overcoming multiple intracellular barriers, including protection against nuclease degradation, transport across cellular and nuclear membranes, and efficient endosomal escape followed by decomplexation of pDNA–vector complexes [24-27]. Previous studies have reported that transfection efficiency in MSCs using transfection methods generally remains in the low to moderate range, thus requiring additional conditions to enhance transfection efficiency [25,28,29]. Moreover, commonly used transfection strategies are often associated with cytotoxic effects, which can reduce cell viability and compromise the therapeutic potential of stem cells [30].

Although transfection strategies have been investigated in MSCs from various tissue sources, transfection efficiency is highly dependent on cell type, plasmid construct, and experimental conditions, limiting the direct applicability of existing protocols to UC-MSCs. In addition, previous optimization studies have predominantly focused on reporter genes rather than therapeutically relevant genes such as BMP-2. Considering the limited endogenous BMP-2 expression in MSCs and the short biological half-life of recombinant BMP-2 protein, this study aimed to systematically optimize transfection BMP-2 gene delivery in UC-MSCs by evaluating transfection reagent type, reagent-to-DNA ratio, and cell passage number to maximize transgene expression while minimizing cytotoxicity. Importantly, this study was designed with a translational perspective toward the development of BMP-2–enriched UC-MSC secretome-based therapeutics for bone regeneration, where preservation of cell viability and biological functionality is critical for therapeutic efficacy.

Materials and methods

Isolation and culture of UC-MSCs

UC-MSCs were isolated from human umbilical cords obtained during caesarean deliveries. All procedures were approved by the Health Research Ethics Committee of the Faculty of Medicine, Universitas Indonesia (Protocol Number: KET-272 UN2.F1/CTIK/PPM.00.02/2024). Briefly, umbilical cord were initially decontaminated by washing with 5% povidone-iodine solution, followed by twice washed with PBS to remove residual blood. The Wharton's jelly was then dissected from the umbilical cord and cut into

small fragments of approximately 2 - 3 mm^3. UC-MSCs were cultured using the explant method, where the tissue fragments were placed onto culture dishes and maintained in α-minimum essential medium (α-MEM) supplemented with platelet-rich plasma (PRP), GlutaMAX™, and antibiotics-antimycotics. The cultures were incubated at 37 °C in a humidified atmosphere containing 5% CO_2, and the culture medium was replaced every 2 - 3 days. Cells were harvested upon reaching approximately 80% - 90% confluence for subsequent experiments.

Plasmid design

The recombinant plasmid used in this study had a total length of 5,649 bp and was designed to drive efficient expression of the human BMP-2 gene in mammalian cells. Gene expression was regulated by a spleen focus-forming virus (SFFV) promoter, which enables strong constitutive transcription. A Kozak consensus sequence was positioned upstream of the BMP-2 coding region to enhance translational efficiency. The construct contained the codon-optimized BMP-2 gene sequence, followed by a simian virus 40 (SV40) late polyadenylation signal to ensure proper transcriptional termination. In addition, a cytomegalovirus (CMV) promoter element was included to support expression of green fluorescent protein (GFP) as a reporter gene. The plasmid also contained bovine growth hormone polyadenylation (BGH pA) signals to improve mRNA stability. For bacterial propagation and selection, the vector carried a plasmid University of California (pUC) origin of replication and an ampicillin resistance gene, allowing plasmid amplification and selection in *Escherichia coli*.

Transfections

UC-MSCs were seeded in 12-well culture plates at a density of 5,000 cells/cm^2 and cultured under standard conditions until reaching approximately 60% - 70% confluence. Prior to transfection, the culture medium was replaced with serum- and antibiotic-free α-MEM to reduce potential interference with the transfection reagents. Plasmid transfection was performed using 3 different reagents, namely polyethyleneimine (PEI), Lipofectamine™ 2000 (Thermo Scientific, 11668027), and Lipofectamine™ 3000 (Thermo Scientific, L3000008), following the manufacturers' instructions. Briefly, plasmid DNA was diluted in Opti-MEM, while each transfection reagent was prepared separately in the same medium. The diluted DNA and reagent solutions were subsequently combined at equal volumes and incubated at room temperature for approximately 15 min to allow the formation of DNA-reagent complexes. The resulting complexes were then added to the cultured cells and incubated under standard culture conditions for 48 h to allow transgene expression. All transfection experiments were performed in triplicate to ensure the reproducibility and reliability of the results.

Analysis of GFP positive signal using flowcytometry

GFP-positive cells were quantified using flow cytometry to evaluate transfection efficiency. At 48 h post-transfection, cells were harvested by trypsinization, collected, and washed with PBS to remove residual medium. Flow cytometric analysis was performed using a BD FACSAria™ III flow cytometer (BD Biosciences, USA) equipped with a 488 nm excitation laser for detection of GFP fluorescence. A minimum of 10,000 events per sample were acquired. Forward scatter (FSC) and side scatter (SSC) parameters were used to gate viable cell populations and exclude cellular debris. GFP-positive cells were identified based on fluorescence intensity detected in the FITC channel relative to non-transfected control cells. The percentage of GFP-positive cells was calculated as an indicator of transfection efficiency. All experiments were conducted in triplicate to ensure reproducibility.

Fluorescence microscopic observation

Cultured cells were examined using a Nikon Eclipse Ni-U fluorescence microscope (Nikon, Japan) to evaluate GFP expression following plasmid transfection. At 48 h post-transfection, clear GFP fluorescence was detected in transfected UC-MSCs, indicating successful plasmid uptake and transgene expression. The GFP-positive cells displayed bright green fluorescence distributed throughout the cytoplasm. In contrast, no detectable fluorescence signal was observed in the non-transfected control group, confirming that the observed fluorescence was specifically associated with plasmid-mediated gene expression.

Viability of cells

Cell viability was determined using the Trypan Blue exclusion assay. Following of 48 h transfection, cells were harvested and resuspended in culture medium. An aliquot of the cell suspension was mixed with 0.4% Trypan Blue solution at a 1:1 ratio. The mixture was then loaded onto a hemocytometer for cell counting under a light microscope. Viable cells, which exclude the dye, were identified as unstained cells, whereas non-viable cells appeared blue due to membrane permeability. The percentage of viable cells was calculated by dividing the number of viable cells by the total number of counted cells and multiplying by 100%.

BMP-2 gene expression analysis

Total RNA was extracted from the samples using the Quick-RNA Miniprep Kit (Zymo Research, R1055) according to the manufacturer's instruction. The concentration of RNA obtained was then used for complementary DNA (cDNA) synthesis, where 1 µg of total RNA was reverse-transcribed using the ReverTra Ace™ qPCR RT Master Mix with gDNA Remover (Toyobo, FSQ-301). Quantitative real-time PCR (qRT-PCR) was subsequently carried out using the SensiFAST™ SYBR™ Lo-ROX Kit (Bioline, BIO-94005) on an Applied Biosystems™ 7500 Real-Time PCR System (Thermo Scientific, USA) to evaluate BMP-2 gene expression. Relative expression levels were determined using the comparative cycle threshold ($\Delta\Delta C_T$ method), with Glyceraldehyde 3-phosphate dehydrogenase (GAPDH) serving as the internal housekeeping gene for normalization. The sequences of the primers used for gene expression analysis are presented in **Table 1**.

Table 1 Primer sequence for qRT-PCR.

Primer	Sequence (5'- 3')
BMP-2 (NM_001200.4)	Forward: GAGAAGGAGGAGGCAAAGAAA Reverse: GAAGCTCTGCTGAGGTGATAAA
GAPDH (NM_001256799.3)	Forward: CAATGACCCCTTCATTGACC Reverse: TTGATTTTGGAGGGATCTCG

BMP-2 protein concentration analysis

BMP-2 protein concentration in the conditioned medium was quantified using an enzyme-linked immunosorbent assay (ELISA). After transfection, the conditioned medium (CM) from cultured cells was collected and centrifuged at 3,500 rpm for 30 min to remove cellular debris. The resulting pellet was discarded, and the supernatant was subsequently filtered through a 0.22 µm membrane filter to ensure sterility and eliminate any remaining particulates. The concentration of secreted BMP-2 in the CM was then determined using a human BMP-2 ELISA kit (Elabscience, E-EL-H0011) according to the manufacturer's instruction. Briefly, standards and samples were added to the ELISA plate, followed by incubation with the appropriate detection reagents. Absorbance was measured at 450 nm using a microplate reader, and BMP-2 concentrations were calculated based on a standard curve generated from known concentrations of BMP-2. All measurements were performed in triplicate to ensure the reliability of the data.

Statistical analysis

Statistical analyses were conducted using GraphPad Prism version 10 (GraphPad Software, USA), with statistical significance defined at $p < 0.05$. The normality of the data distribution was evaluated using the Shapiro-Wilk test, while homogeneity of variance was assessed using Levene's test. For datasets that satisfied these assumptions, statistical comparisons were performed using one-way analysis of variance (ANOVA) followed by Tukey's post hoc test, and the results are presented as mean ± standard deviation (SD). In contrast, datasets that did not meet the normality or variance assumptions were analyzed using the Kruskal-Wallis test, followed by Mann-Whitney U tests for pairwise comparisons.

Results and discussion

Evaluation of transfection optimalization following transfection reagents

Bright-field microscopy revealed that cells in all experimental groups retained the characteristic spindle-shaped morphology typical of MSCs (**Figure 1(a)**). However, a modest decrease in cell density was observed in the Lipo 3,000 group, suggesting the presence of mild cytotoxic effects associated with the transfection reagent. Quantitative analysis showed that cell viability in the Lipo 3,000 group averaged approximately 86%, which was significantly lower than that of the untreated control group (mean viability: 95%) (**Figure 1(e)**). Despite this reduction, the observed viability remained relatively high and within an acceptable range for transfection experiments. Notably, previous studies have reported more pronounced cytotoxicity, where MSCs transfected with Lipofectamine™ LTX exhibited a progressive decline in viability to around 60% by day seven post-transfection [31].

Fluorescence microscopy demonstrated that GFP-positive signals were observed only in the Lipo 3,000 group (**Figure 1(b)**). This observation was further confirmed by flow cytometry analysis, which similarly detected GFP expression exclusively in cells transfected with Lipo 3,000 (**Figure 1(c)**). Quantitative analysis of GFP-positive cell populations showed that Lipo 3,000 produced the highest transfection efficiency, reaching approximately 9% - 10%, whereas the PEI and Lipo 2,000 groups exhibited minimal transfection efficiency of less than 1% (**Figure 1(d)**). Similar trends were observed at both the transcriptional and protein levels. qRT-PCR results revealed that BMP-2 mRNA expression was highest in the Lipo 3,000 group, showing an approximately 2.4-fold increase compared with the other experimental groups (**Figure 1(f)**). Consistently, ELISA analysis demonstrated that BMP-2 protein secretion also reached the highest level in this group, with a concentration of 261.4 pg/mL (**Figure 1(g)**). These findings indicate that Lipofectamine™ 3000 provides superior performance in delivering plasmid DNA into UC-MSCs and promoting the expression of both GFP and BMP-2 compared with the other transfection reagents evaluated in this study.

The superior transfection performance of Lipofectamine™ 3000 observed in this study can be attributed to its advanced lipid nanoparticle formulation, which incorporates an additional P3000™ reagent that enhances DNA compaction and reduces the overall surface charge of the lipoplex complex. This modification results in a more favorable physicochemical profile, characterized by reduced aggregation tendency and improved colloidal stability, which collectively facilitate more efficient cellular uptake via clathrin-mediated endocytosis [32]. Furthermore, the inclusion of the P3000™ reagent has been demonstrated to reduce non-specific protein adsorption onto the lipoplex surface, thereby minimizing immune recognition and prolonging intracellular trafficking toward the nucleus [33]. In contrast, Lipofectamine™ 2000 relies on a cationic lipid formulation without such modifications, rendering it more susceptible to serum-induced aggregation and charge neutralization under standard cell culture conditions, which may account for its diminished performance in the present study [34]. A similar outcome was observed for PEI, which, despite being well recognized for its capacity to condense DNA effectively and its proton sponge effect that facilitates endosomal escape, has also been associated with considerable cytotoxicity in various cell types [35]. The molecular weight of PEI, typically ranging from 25 to 40 kDa, has been shown to influence the formation of DNA complexes in a manner that concurrently elevates cellular toxicity and compromises transfection efficiency [36]. Consistent with this, even in cancer cell lines PEI-mediated transfection efficiency has been reported to reach only 10% [37].

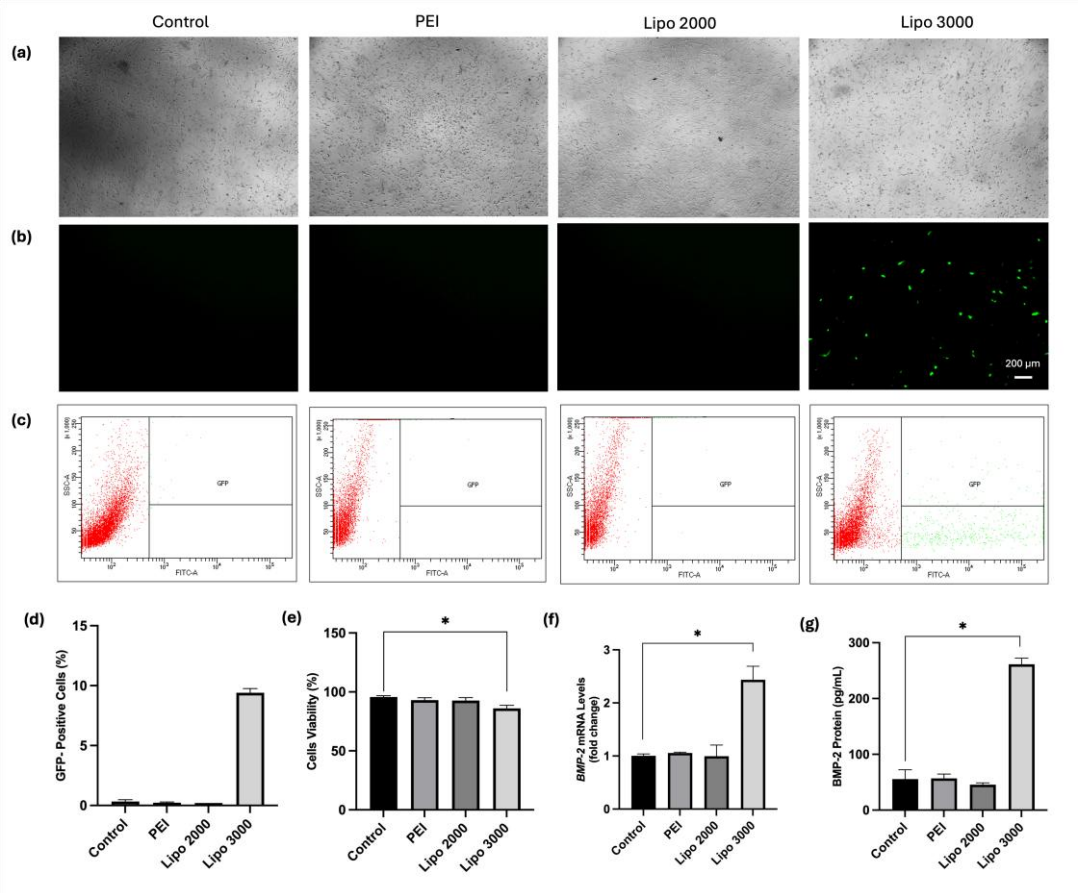


Figure 1 Evaluation of transfection optimalization following transfection reagents. (a) Bright-field microscopy images showing cell morphology across all groups at 48 h post-transfection. (b) Fluorescence microscopy images demonstrating GFP expression as an indicator of successful plasmid delivery. (c) Representative flow cytometry scatter plots showing the GFP-positive cell population in each group. (d) Quantification of GFP-positive cells (%) as determined by flow cytometry analysis. (e) Cell viability (%) assessed following transfection across all groups. (f) Relative BMP-2 mRNA expression levels quantified by qRT-PCR, presented as fold change relative to the control group. (g) BMP-2 protein concentration (pg/mL) measured in the conditioned medium cells by ELISA. Data are presented as mean ± standard deviation (SD). Asterisk (*) indicates statistically significant difference compared to the control group ($p < 0.05$).

Evaluation of transfection optimalization following Reagent-to-DNA ratios

After identifying Lipofectamine™ 3000 as the most effective transfection reagent, further experiments were performed to determine the optimal reagent-to-DNA ratio for BMP-2 plasmid delivery in UC-MSCs. A constant volume of Lipofectamine™ 3000 (4.5 µL) was combined with four different amounts of plasmid DNA: 1.25 µg (Ratio 1), 2.5 µg (Ratio 2), 5 µg (Ratio 3), and 10 µg (Ratio 4) (**Figure 2(a)**). Bright-field microscopy showed that the typical MSC morphology was maintained across all ratio groups, with no visible signs of cellular damage or detachment (**Figure 2(b)**). Fluorescence microscopy revealed GFP expression in all transfected groups, with the strongest fluorescence signal observed in Ratio 2, followed by Ratio 3, Ratio 1, and Ratio 4 (**Figure 2(c)**). These observations were supported by flow cytometry analysis, which quantified GFP-positive cell populations at approximately 2.7%, 9.0%, 6.5%, and 3.0% for Ratios 1 - 4 (**Figures 2(d) - 2(e)**). Statistical analysis confirmed that the transfection efficiency achieved with Ratio 2 was significantly higher than that of the other groups ($p < 0.05$), suggesting that 2.5 µg of plasmid DNA represents the optimal DNA input for Lipofectamine 3000™–mediated transfection in UC-MSCs under the tested conditions. Consistent with these findings, functional analyses further supported the superiority of Ratio 2. qRT-PCR results demonstrated the highest BMP-2 mRNA expression in this group, reaching

approximately a 2.7-fold increase relative to the other experimental groups (**Figure 2(g)**). Similarly, ELISA analysis showed that BMP-2 protein secretion was also highest in Ratio 2, with a concentration of approximately 245 pg/mL (**Figure 2(h)**). These results indicate that the combination of 4.5 µL Lipofectamine™ 3000 with 2.5 µg plasmid DNA represents the optimal transfection condition for BMP-2 delivery in UC-MSCs.

MSCs have been recognized as highly sensitive to transfection conditions, such that small variations in the DNA-to-reagent ratio or reagent concentration can significantly affect both transgene expression levels and cell viability [25]. The observed decline in transfection efficiency at higher DNA concentrations (Ratio 3 and Ratio 4) can be attributed to the imbalance between the lipid carrier and DNA, which leads to the formation of oversized or poorly structured lipoplex complexes with suboptimal physicochemical properties for cellular uptake [38,39]. It has been well established that the charge ratio between the cationic lipid and anionic DNA is a critical determinant of lipoplex size, zeta potential, and transfection efficiency [38,40]. When DNA is present in excess relative to the lipid carrier, the net surface charge of the complex shifts toward neutral or negative values, reducing electrostatic interactions with the negatively charged cell membrane and impairing endocytosis-mediated cellular uptake [41,42]. Conversely, insufficient DNA input, as observed in Ratio 1, results in suboptimal transgene dosage per cell despite adequate complex formation, ultimately limiting gene expression levels [43].

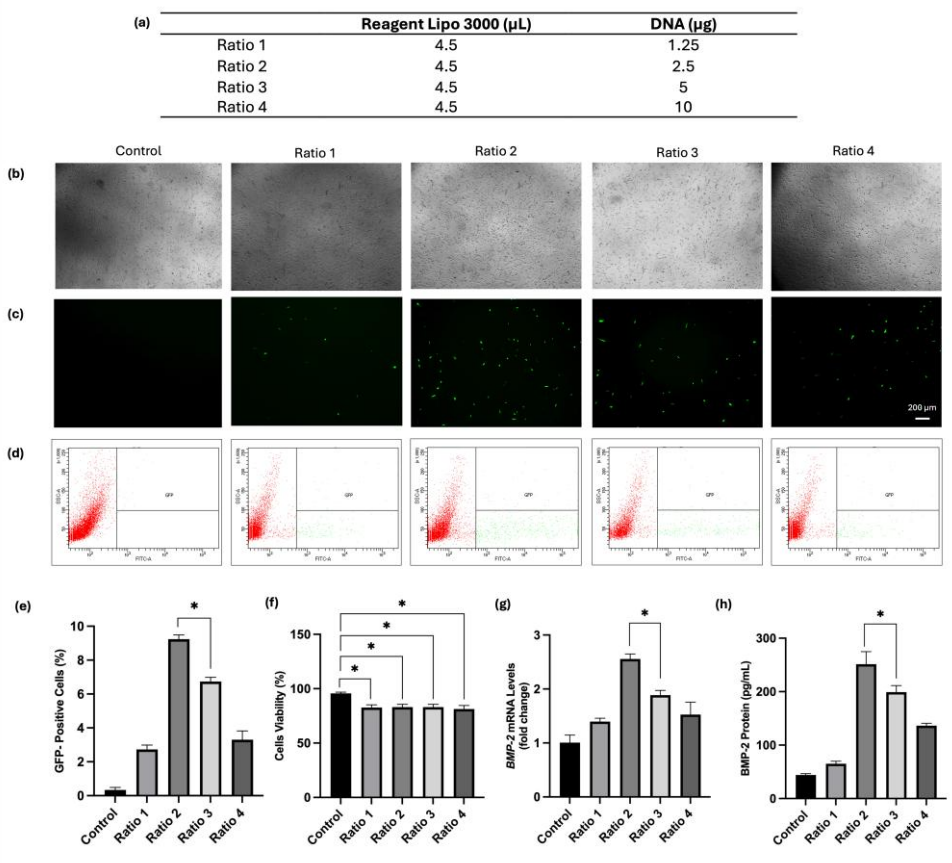


Figure 2 Evaluation of transfection optimalization following reagent-to-DNA ratios. (a) Summary table of Lipofectamine 3000™ volume and DNA amount used for each transfection ratio. (b) Bright-field microscopy images showing cell morphology across all groups at 48 h post-transfection. (c) Fluorescence microscopy images demonstrating GFP expression as an indicator of successful plasmid delivery across all ratio groups. (d) Representative flow cytometry scatter plots showing the GFP-positive cell population in each group. (e) Quantification of GFP-positive cells (%) as determined by flow cytometry analysis. (f) Cell viability (%) assessed following transfection across all ratio groups. (g) Relative BMP-2 mRNA expression levels quantified by qRT-PCR, presented as fold change relative to the control group. (h) BMP-2 protein concentration (pg/mL) measured in the conditioned medium cells by ELISA. Data are presented as mean ± standard deviation (SD). Asterisk (*) indicates statistically significant difference between indicated groups ($p < 0.05$).

Evaluation of transfection optimalization following cell passage numbers

Bright-field microscopy revealed that UC-MSCs maintained a typical spindle-shaped morphology across all passage groups, with no noticeable morphological differences observed among Passages 2, 4, 6, and 8 (**Figure 3(a)**). Observations from fluorescence microscopy (**Figure 3(b)**) and flow cytometry analysis (**Figures 3(c) - 3(d)**) revealed that GFP expression was highest in cells at Passage 2 (9.8 ± 0.6%) and gradually decreased with increasing passage number, reaching significantly lower levels at Passages 6 and 8 (3.2 ± 0.4% and 2.4 ± 0.3%, respectively; $p < 0.05$). Although transfection efficiency declined with higher passages, cell viability remained relatively stable across all groups, ranging between 80% and 84%, with no statistically significant differences observed between Passages 2 and 8 ($p > 0.05$; **Figure 3(e)**). These findings suggest that the reduction in GFP expression was not primarily caused by cytotoxicity. In agreement with this trend, qRT-PCR analysis showed that BMP-2 mRNA expression was highest at Passage 2 (2.61 ± 0.14-fold relative to control) and progressively decreased at later passages, with significantly lower expression detected at Passages 6 and 8 (1.52 ± 0.09 and 1.48 ± 0.10-fold, respectively; $p < 0.05$; **Figure 3(f)**). A comparable pattern was also observed at the protein level, where ELISA results demonstrated that BMP-2 secretion peaked at Passage 2 (248.6 ± 18.3 pg/mL) and significantly declined at Passages 6 and 8 (152.1 ± 11.4 pg/mL and 129.8 ± 9.6 pg/mL, respectively; $p < 0.05$; **Figure 3(g)**).

Overall, these results demonstrate a passage-dependent decrease in transfection efficiency and transgene expression in MSCs, while maintaining relatively stable cell viability. Cell passage number was also identified as a significant biological factor influencing transfection efficiency in UC-MSCs. Cells at lower passages consistently demonstrated higher transfection efficiency compared to the higher passages. MSCs expansion at higher passage tends to undergo cellular senescence, variation in genetic stability, and short lifespan [44]. In serially passaged MSCs, the onset of senescence is accompanied by progressive changes in mitochondrial dynamics, decreased mitochondrial membrane potential, increased ROS production, and reduced cellular antioxidant capacity [45]. It has been reported that the lower passage MSCs exhibit greater metabolic and proliferative activity, making them inherently more receptive to gene delivery than the higher passage MSCs [46,47]. Transfection efficiency is also strongly influenced by cell cycle activity. In the group with the highest transfection efficiency (low-passage MSCs), high cell division activity increases the chance of exogenous DNA entering the nucleus during the mitosis phase, when the nuclear envelope is transiently disrupted [24]. Conversely, at higher passage numbers, reduced cell division activity and increased cell cycle arrest diminish the probability of exogenous DNA reaching the nucleus [25]. Furthermore, at higher passages, changes in cytoskeleton structure and increased stability of endosomal vesicles can inhibit the movement of DNA complexes within the cytoplasm and slow the endosomal escape process [48].

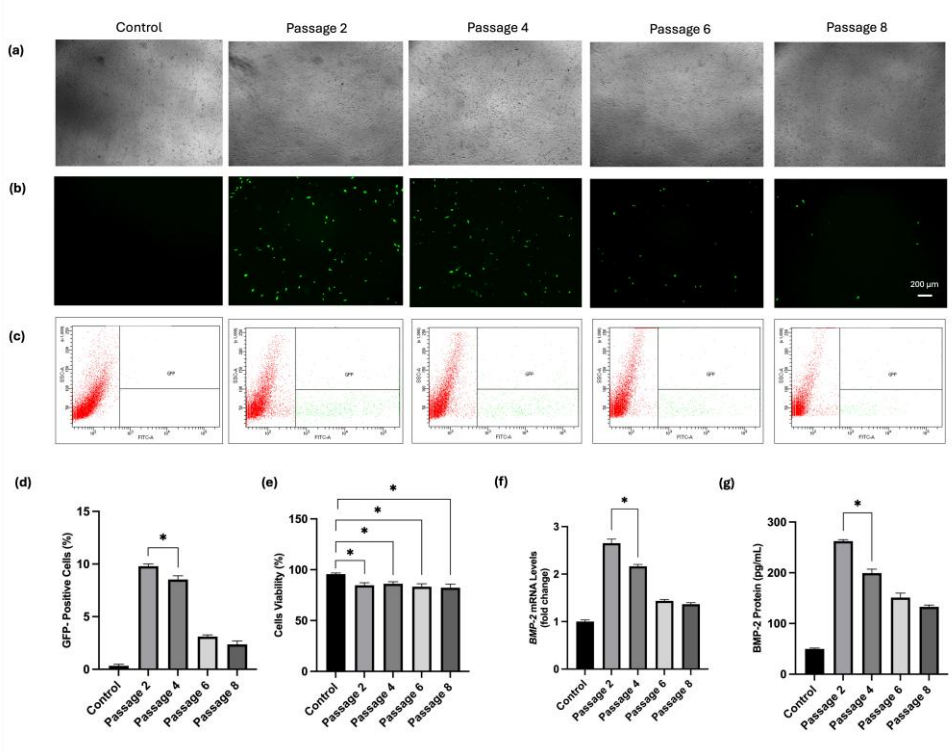


Figure 3 Evaluation of transfection optimalization following cells passage numbers. (a) Bright-field microscopy images showing cell morphology at each passage number at 48 h post-transfection. (b) Fluorescence microscopy images demonstrating GFP expression as an indicator of successful plasmid delivery across all passage groups. (c) Representative flow cytometry scatter plots showing the GFP-positive cell population at each passage number. (d) Quantification of GFP-positive cells (%) as determined by flow cytometry analysis across passage groups. (e) Cell viability (%) assessed following transfection at each passage number. (f) Relative BMP-2 mRNA expression levels quantified by qRT-PCR, presented as fold change relative to the control group. (g) BMP-2 protein concentration (pg/mL) measured in the conditioned medium cells by ELISA. Data are presented as mean ± standard deviation (SD). Asterisk (*) indicates statistically significant difference between indicated groups ($p < 0.05$).

Optimum conditions for UC-MSCs transfection

The optimization of transfection conditions in UC-MSCs was performed using Lipofectamine™ 3000 with a ratio of 4.5 µL reagent to 2.5 µg plasmid DNA at passage 2. Under these conditions, the cells maintained their characteristic MSC phenotype, as confirmed by flow cytometry analysis. Prior to transfection, UC-MSCs exhibited high expression of positive MSC markers, including CD73 (99.9%), CD90 (100%), and CD105 (99.5%), with minimal expression of negative markers (0.3%). These results indicate a highly pure MSC population consistent with the standard criteria for MSC identification. Following transfection under the optimized conditions, the expression of CD73 (99.5%) and CD90 (99.8%) remained stable, demonstrating that the selected Lipofectamine™ 3000 ratio did not significantly affect the core phenotypic identity of the cells. A slight reduction in CD105 expression (93.8%) was observed, which may reflect transient cellular stress induced by the transfection process or temporary modulation of surface protein expression.

In this study, BMP-2 protein was successfully secreted by transfected UC-MSCs under optimized transfection conditions, demonstrating enhanced transgene expression while preserving cellular characteristics and viability. These findings highlight the potential application of BMP-2–enriched UC-MSC secretome as a promising therapeutic strategy for bone regeneration. Compared with recombinant BMP-2 therapy, secretome-based delivery may provide more sustained osteogenic activity while overcoming limitations associated with short protein half-life and repeated administration. Moreover, gene delivery

approaches such as lipid-based transfection offer favorable safety profiles for translational applications due to their lower risks of insertional mutagenesis and immunogenicity. Alternative approaches, including electroporation, may also be considered depending on the required transgene stability and expression duration, particularly for sustained BMP-2 production. Further studies evaluating transgene stability, biosafety, and therapeutic efficacy are required to support the clinical translation of MSC secretome-based gene therapy for bone regeneration.

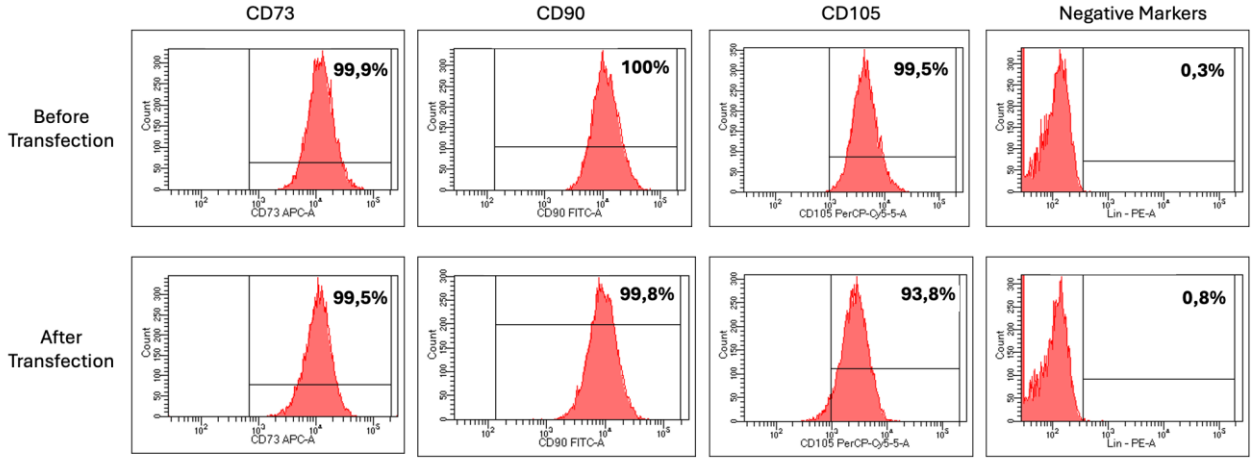


Figure 4 Immunophenotypic characterization of UC-MSCs before and after transfection. Flow cytometry histograms showing expression of MSC positive markers (CD73, CD90, CD105) and negative lineage markers (Lin-) before (upper panel) and after (lower panel) transfection. High expression of positive markers and minimal negative marker expression were maintained in both conditions, confirming preserved mesenchymal identity of UC-MSCs following transfection. Data presented in mean, n=3. (CD: Cluster of differentiation, APC-A: Allophycocyanin – Area, FITC-A: Fluorescein Isothiocyanate – Area, PerCP-Cy5.5-A: Peridinin Chlorophyll Protein–Cyanine 5.5 – Area, PE-A: Phycoerythrin – Area).

Conclusions

In conclusion, this study demonstrates that optimizing transfection conditions using Lipofectamine™ 3000 at a ratio of 4.5 µL to 2.5 µg DNA in passage 2 UC-MSCs effectively enhances BMP-2 expression and secretion while preserving cell viability and phenotypic stability. The optimized parameters were able to overcome the inherent resistance of MSCs to transfection, resulting in improved gene delivery without compromising the defining characteristics of the cells. These findings highlight the importance of carefully balancing transfection efficiency and cytocompatibility in primary stem cells. Overall, this approach provides a reliable and reproducible strategy to enhance the therapeutic potential of UC-MSCs, supporting their application in bone regeneration and the development of MSC-based or secretome-based regenerative therapies.

Acknowledgements

The authors thank to DIPI Small Research Grant 2025 awarded to the author NFM to support this research. The research were financially funded by Q2 Scheme Research Grant named Hibah Publikasi Terindeks Internasional (PUTI Q2 2023) from the Directorate of Research and Development, Universitas Indonesia awarded to *IHD*.

Ethics approval and consent to participate

This study was reviewed and approved by the Health Research Ethics Commitee-Faculty of Medicine Universitas Indonesia, Jawa Barat 16424, Indonesia under the approval number KET-272 UN2.F1/CTIK/PPM.00.02/2024. Informed consent from umbilical cord donors was obtained prior to sample collection, in accordance with ethical guidelines and regulations.

Declaration of Generative AI in Scientific Writing

During the preparation of this manuscript, the authors used generative artificial intelligence (AI) tools (e.g., ChatGPT by OpenAI, Claude, and QuillBot) to assist with language refinement, grammar correction, and structuring of the text. No AI tools were used to generate, analyze, or interpret scientific data. All outputs were carefully reviewed, validated, and edited by the authors, who take full responsibility for the accuracy, integrity, and originality of the work.

CRediT Author Statement

Nuzli Fahdia Mazfufah: Conceptualization; Methodology; Investigation; Formal Analysis; Data Curation; Writing – Original Draft; Visualization. **Retno Wahyu Nurhayati**: Supervision; Conceptualization; Methodology; Writing – Review & Editing; Validation. **Maulana Dias Pratama**: Investigation; Data Curation; Writing – Original Draft. **Ismail Hadisoebroto Dilogo**: Supervision; Conceptualization; Resources; Funding Acquisition. **Delvac Oceandy**: Supervision; Conceptualization; Validation.

References

[1] JW Łuczak, M Palusińska, D Matak, D Pietrzak, P Nakielski, S Lewicki, M Grodzik and Ł Szymański. The future of bone repair: Emerging technologies and biomaterials in bone regeneration. *International Journal of Molecular Sciences* 2024; **25(23)**, 12766.

[2] J Quek, C Vizetto-Duarte, SH Teoh and Y Choo. Towards stem cell therapy for critical-sized segmental bone defects: Current trends and challenges on the path to clinical translation. *Journal of Functional Biomaterials* 2024; **15(6)**, 145.

[3] F Schulze, A Lang, J Schoon, GI Wassilew and J Reichert. Scaffold guided bone regeneration for the treatment of large segmental defects in long bones. *Biomedicines* 2023; **11(2)**, 325.

[4] PL Rodham, VP Giannoudis, NK Kanakaris and PV Giannoudis. Biological aspects to enhance fracture healing. *EFORT Open Reviews* 2023; **8(5)**, 264-282.

[5] S Law and S Chaudhuri. Mesenchymal stem cell and regenerative medicine: Regeneration versus immunomodulatory challenges. *American Journal of Stem Cells* 2013; **2(1)**, 22-38.

[6] K Zha, Y Tian, AC Panayi, B Mi and G Liu. Recent advances in enhancement strategies for osteogenic differentiation of mesenchymal stem cells in bone tissue engineering. *Frontiers in Cell and Developmental Biology* 2022; **10**, 824812.

[7] MY Artamonov and EL Sokov. Intraosseous delivery of mesenchymal stem cells for the treatment of bone and hematological diseases. *Current Issues in Molecular Biology* 2024; **46(11)**, 12672-12693.

[8] S Chetty, R Yarani, G Swaminathan, R Primavera, S Regmi, S Rai, J Zhong, A Ganguly and AS Thakor. Umbilical cord mesenchymal stromal cells-from bench to bedside. *Frontiers in Cell and Developmental Biology* 2022; **10**, 1006295.

[9] M Hussein. Advancing regenerative therapies with umbilical cord-derived mesenchymal stem cells: A review. *Biomolecules and Biomedicine* 2025; **26(4)**, 537-546.

[10] S Moghadasi, M Elveny, HS Rahman, W Suksatan, AT Jalil, WK Abdelbasset, AV Yumashev, S Shariatzadeh, R Motavalli, F Behzad, F Marofi, A Hassanzadeh, Y Pathak and M Jarahian. A paradigm shift in cell-free approach: The emerging role of MSCs-derived exosomes in regenerative medicine. *Journal of Translational Medicine* 2021; **19**, 302.

[11] CM Trigo, JS Rodrigues, SP Camões, S Solá and JP Miranda. Mesenchymal stem cell secretome for regenerative medicine: Where do we stand? *Journal of Advanced Research* 2025; **70**, 103-124.

[12] B Torrecillas-Baena, V Pulido-Escribano, G Dorado, MÁ Gálvez-Moreno, M Camacho-Cardenosa and A Casado-Díaz. Clinical potential of mesenchymal stem cell-derived exosomes in bone regeneration. *Journal of Clinical Medicine* 2023; **12(13)**, 4385.

[13] A Lotfy, NM AboQuella and H Wang. Mesenchymal stromal/stem cell (MSC)-derived exosomes in clinical trials. *Stem Cell Research & Therapy* 2023; **14**, 66.

[14] J Cheng, Y Sun, Y Ma, Y Ao, X Hu and Q Meng. Engineering of MSC-derived exosomes: A promising cell-free therapy for osteoarthritis. *Membranes* 2022; **12(8)**, 739.

[15] MCDCP Cestari, RF Tovo and DF Bueno. MSC-derived secretome and exosomes in dermatology: Mechanisms, therapeutic opportunities, and scientific challenges-a narrative review. *International Journal of Dermatology* 2026; **65(2)**, 257-272.

[16] IH Dilogo, J Fiolin, AF Canintika, JA Pawitan and E Luviah. The effect of secretome, xenogenic bone marrow-derived mesenchymal stem cells, bone morphogenetic protein-2, hydroxyapatite granule and mechanical fixation in critical-size defects of rat models. *Archives of Bone and Joint Surgery* 2022; **10(1)**, 17-22.

[17] JB Lee, JY Hong, H Shim, S Kim, DW Lee, B Kwon and JH Yun. Bone morphogenetic protein-2-derived osteogenic peptide promotes bone regeneration via osteoblastogenesis. *Regenerative Therapy* 2025; **30**, 911-919.

[18] R Taday, P Jungbluth, S Zensen, T Krakau, J Windolf, MJ Hoffmann and V Grotheer. BMP-2-driven osteogenesis: A comparative analysis of porcine BMSCs and ASCs and the role of TGF-β and FGF signaling. *Biology* 2025; **14(6)**, 610.

[19] X Chen, B Tan, Z Bao, S Wang, R Tang, Z Wang, G Chen, S Chen, WW Lu, D Yang and S Peng. Enhanced bone regeneration via spatiotemporal and controlled delivery of a genetically engineered BMP-2 in a composite hydrogel. *Biomaterials* 2021; **277**, 121117.

[20] JH Lee, JH Youn, HJ Park and SJ Hyun. Low-dose bone morphogenetic protein use in spinal fusion: Rethinking clinical efficacy. *Journal of Korean Neurosurgical Society* 2025; **68(6)**, 632-643.

[21] NF Mazfufah, IH Dilogo, RW Nurhayati, D Oceandy, ST Widyaningtyas, MD Pratama and G Jang. Genetic engineering of umbilical cord-derived mesenchymal stem cells to enhance BMP-2 secretion via signal peptide optimization. *Biomedicines* 2026; **14(1)**, 76.

[22] F Li, J Wu, D Li, L Hao, Y Li, D Yi, KWK Yeung, D Chen, WW Lu, H Pan, TM Wong and X Zhao. Engineering stem cells to produce exosomes with enhanced bone regeneration effects: An alternative strategy for gene therapy. *Journal of Nanobiotechnology* 2022; **20**, 135.

[23] JA Pawitan, TA Bui, W Mubarok, RD Antarianto, RW Nurhayati, IH Dilogo and D Oceandy. Enhancement of the therapeutic capacity of mesenchymal stem cells by genetic modification: A systematic review. *Frontiers in Cell and Developmental Biology* 2020; **8**, 587776.

[24] S Huang, TR Henderson, CD Soeandy, A Lezhanska and JT Henderson. An efficient low cost means of biophysical gene transfection in primary cells. *Scientific Reports* 2024; **14**, 13179.

[25] S Christoffers, L Seiler, E Wiebe and C Blume. Possibilities and efficiency of MSC co-transfection for gene therapy. *Stem Cell Research & Therapy* 2024; **15**, 150.

[26] R Allen and T Yokota. Endosomal escape and nuclear localization: Critical barriers for therapeutic nucleic acids. *Molecules* 2024; **29(24)**, 5997.

[27] S Honrath, M Burger and JC Leroux. Hurdles to healing: Overcoming cellular barriers for viral and nonviral gene therapy. *International Journal of Pharmaceutics* 2025; **674**, 125470.

[28] Y Jin, G Han, Y Gao, H Cheng, C Sun, J Ni, J Zhou, H Zhang and Y Ding. Serum-tolerant polymeric complex for stem-cell transfection and neural differentiation. *Nature Communications* 2025; **16**, 2022.

[29] S Noske, M Karimov, M Hansen, N Zatula, A Ewe and A Aigner. Non-viral siRNA transfection of primary mesenchymal stromal cells (MSCs): Assessment of tyrosine-modified PEI and PPI efficacy and biocompatibility. *International Journal of Pharmaceutics* 2022; **612**, 121359.

[30] R Ojha, E Timin, L Szirovicza, W Xu and J Hepojoki. A systematic comparison of in-house prepared transfection reagents in the delivery of mRNA or DNA to a wide range of cultured cells. *Journal of Biological Chemistry* 2025; **301(12)**, 110742.

[31] M Taghavi, A Parham, H Dehghani and H Naderi-Meshkin. Optimizing Lipofectamine LTX complex and G-418 concentration for improvement of transfection efficiency in human mesenchymal stem cells. *Archives of Razi Institute* 2021; **76(5)**, 1315-1325.

[32] CDT Runzer, S Anand, C Mota, L Moroni, C Plank, M van Griensven and ER Balmayor. Cellular uptake of modified mRNA occurs via caveolae-mediated endocytosis, yielding high

protein expression in slow-dividing cells. *Molecular Therapy: Nucleic Acids* 2023; **32**, 960-979.

[33] E Voke, ML Arral, HJ Squire, TJ Lin, R Coreas, A Lui, AT Iavarone, RL Pinals, KA Whitehead and MP Landry. Protein corona formed on lipid nanoparticles compromises delivery efficiency of mRNA cargo. *Nature Communications* 2025; **16**, 8699.

[34] Z Jahanafrooz, B Bakhshandeh and E Shirzadi. Comparative evaluation of Lipofectamine and dendrimer for transfection of short RNA into human T47D and MCF-10A cell lines. *Advanced Pharmaceutical Bulletin* 2023; **13(2)**, 385-392.

[35] J Casper, SH Schenk, E Parhizkar, P Detampel, A Dehshahri and J Huwyler. Polyethylenimine (PEI) in gene therapy: Current status and clinical applications. *Journal of Controlled Release* 2023; **362**, 667-691.

[36] H Wang, X Liu, X Ai, KC Remant-Bahadur, TA Dick, B Yan, T Lu, X Zhou, R Luo, M Liu, X Wang, K Li, W Wang, H Uludag and W Fu. Safe and effective delivery of mRNA using modified PEI-based lipopolymers. *Pharmaceutics* 2023; **15(2)**, 410.

[37] S Yang, Q Zhang, Y Zhuang, J Li and X Fu. Plate centrifugation enhances the efficiency of polyethylenimine-based transfection and lentiviral infection. *Journal of Virological Methods* 2024; **330**, 115039.

[38] D Pozzi and G Caracciolo. Looking back, moving forward: Lipid nanoparticles as a promising frontier in gene delivery. *ACS Pharmacology & Translational Science* 2023; **6(11)**, 1561-1573.

[39] H Tae, S Park, LY Tan, C Yang, YA Lee, Y Choe, T Wüstefeld, S Jung and NJ Cho. Elucidating structural configuration of lipid assemblies for mRNA delivery systems. *ACS Nano* 2024; **18(17)**, 11284-11299.

[40] S Meinhard, F Erdmann, H Lucas, M Krabbes, S Krüger, C Wölk and K Mäder. T14diLys/DOPE liposomes: An innovative option for siRNA-based gene knockdown? *Pharmaceutics* 2024; **17(1)**, 25.

[41] F Zhao, D Nayyar, YS Hwang, R Bartucci and A Salvati. Effect of positive charges on liposome stability, uptake efficacy and impact on cells. *International Journal of Pharmaceutics* 2025; **681**, 125881.

[42] J Shi, JL Choi, B Chou, RN Johnson, JG Schellinger and SH Pun. Effect of polyplex morphology on cellular uptake, intracellular trafficking, and transgene expression. *ACS Nano* 2013; **7(12)**, 10612-10620.

[43] A Carreño, R Guerrero-Yagüe, E Casal, R Mendoza and JL Corchero. Tuning plasmid DNA amounts for cost-effective transfections of mammalian cells: When less is more. *Applied Microbiology and Biotechnology* 2024; **108**, 98.

[44] SN Rajput, BK Naeem, A Ali, A Salim and I Khan. Expansion of human umbilical cord derived mesenchymal stem cells in regenerative medicine. *World Journal of Stem Cells* 2024; **16(4)**, 410-433.

[45] B Casorati, I Zafferri, S Castiglioni and JA Maier. Replicative senescence in mesenchymal stem cells: An *in vitro* study on mitochondrial dynamics and metabolic alterations. *Antioxidants* 2025; **14(4)**, 446.

[46] L Fang, G Ravindran, ME Al-Masawa, N Mohamad-Fauzi, MS Seghayat, A Salsabila and P Hafez. Immunophenotypic characterization and clinical relevance of passage number in umbilical cord mesenchymal stromal cells: A review. *Cell Transplantation* 2026; **35**, 9636897261433504.

[47] N Carballo-Pedrares, F Ponti, J Lopez-Seijas, D Miranda-Balbuena, N Bono, G Candiani and A Rey-Rico. Non-viral gene delivery to human mesenchymal stem cells: A practical guide towards cell engineering. *Journal of Biological Engineering* 2023; **17**, 49.

[48] E Momotyuk, N Ebrahim, K Shakirova and E Dashinimaev. Role of the cytoskeleton in cellular reprogramming: Effects of biophysical and biochemical factors. *Frontiers in Molecular Biosciences* 2025; **12**, 1538806.